ISBN: 978-3-95450-261-5 ISSN: 2673-7000 doi: 10.18429/JACoW-NAPAC2025-WEYN03

# MEASUREMENTS OF ULTRALOW EMITTANCE AND TRANSVERSE COHERENCE AT THE ADVANCED PHOTON SOURCE UPGRADE STORAGE RING*

K. P. Wootton†, X. Shi, Argonne National Laboratory, Lemont, IL, USA



*Abstract*

Recent electron storage ring light sources continue to push towards increasingly lower electron beam sizes. In the present work, we report on the measurements of the electron beam emittance (sub 50 pm rad) achieved at the Advanced Photon Source Upgrade (APS–U), as well as its standing among electron storage ring light sources. We include a brief status update on the beam size monitor beamline at the APS–U. We conclude with a survey of measurement techniques and recent results across multiple laboratories.

## INTRODUCTION

The Advanced Photon Source Upgrade (APS-U) project is a major upgrade to the Advanced Photon Source synchrotron light source facility [1]. With the completion of installation and commissioning of the electron storage ring [2], the goal of the present work was the characterisation of the electron beam size and emittance in the storage ring.

In the present work, we outline three measurement techniques performed during different stages of accelerator commissioning of the APS-U electron storage ring. We describe measurements using a white-beam pinhole camera, monochromatic hard X-ray coherence, and monochromatic soft X-ray undulator radiation characterisation. We outline the status of the beam size monitor beamline, and compare with other recent results from similar laboratories.

## EXPERIMENTS

### *X-ray Pinhole Camera Measurements*

During commissioning of the storage ring for the APS-U, the nominal 38-AM beam size monitor beamline was unavailable. The principal long-term purpose of the 35-BM X-ray beamline configuration is to preserve X-ray beam transport from the 35-BM-A through to 35-BM-C hutches, for use with the bunch purity monitor diagnostic [3, 4]. However the beamline can also be used as-configured for an X-ray pinhole camera for beam size measurements. We propose to measure the electron beam size using a polychromatic X-ray pinhole camera at the 35-BM beamline [5].

In the present work, we outline the components of the pinhole camera used to measure electron beam size at 35-BM [6]. We summarise the results of beam size measurements, and calculate a value for the horizontal emittance.

The root-mean-square (RMS) transverse dimension of the electron beam $\sigma_\mathrm{i}$ can be expressed by:

$$\sigma_\mathrm{i} = \sqrt{\beta_\mathrm{i}\varepsilon_\mathrm{i} + \eta_\mathrm{i}^2\left(\frac{\Delta E}{E}\right)^2}, \quad (1)$$

where $\beta_\mathrm{i}$ is the beta function, $\varepsilon_\mathrm{i}$ the emittance, $\eta_\mathrm{i}$ the dispersion in the coordinate plane $i$, and $\frac{\Delta E}{E}$ the electron beam energy spread. Parameters of the electron beam and pinhole camera in the horizontal plane are summarised in Table 1.

Table 1: Design 35-BM Pinhole Camera Parameters

| Parameter | Symbol | Value |
|---|---|---|
| Beta function | $\beta_x$ | 0.84 m |
| Emittance | $\varepsilon_x$ | 42 pm rad |
| Energy spread | $\frac{\Delta E}{E}$ | 0.156% |
| Dispersion | $\eta_x$ | 3.67 mm |
| Beam size (source) | $\sigma_x$ | 8.3 µm |
| Pinhole magnification | $M$ | 0.832 |
| Beam size (scintillator) | $\Sigma_x$ | 6.9 µm |

Four blades of white-beam slits ($z = 25.0$ m) can be closed to form a rectangular pinhole aperture. A scintillator and optical microscope can be positioned near the end of the beamline ($z = 45.8$ m) in order to image the electron beam in the APS-U storage ring with an X-ray pinhole magnification $20.8/25.0 = 0.832$.

We anticipate that the spatial resolution needed to image an X-ray spot size of Gaussian distribution $\Sigma_x = 6.9\,\mu$m is challenging, but not beyond technical feasibility. For the temporary pinhole camera at 35-BM, we used an Optique Peter white beam x-ray optical microscope system. The key components of the optical microscope included:

- Thin Lutetium Aluminium Garnet - LuAG(Ce) scintillator crystal (~25 µm),
- Optique Peter long working-distance microscope,
- FLIR Blackfly S Digital Camera.

Using this FLIR digital camera (4.8 µm detector pixel pitch), we measured the effective pixel size at the position of the scintillator to be 0.47 µm in both the horizontal and vertical directions.

During early commissioning in 2024, the smallest beam size was measured on May 31, 2024. The accelerator was operated in swap-out mode, maintaining a stored beam current of ~30 mA. The measured and fitted beam profile is plotted

* Work was supported by the U.S. DOE Office of Science-Basic Energy Sciences, under Contract No. DEAC02-06CH11357.
† kwootton@anl.gov

ISBN: 978-3-95450-261-5 ISSN: 2673-7000 doi: 10.18429/JACoW-NAPAC2025-WEYN03

in Fig. 1. The fitted width at the location of the scintillator is $\Sigma_x = 12.4 \pm 0.4\,\mu\text{m}$. Using the pinhole magnification of 0.832, this corresponds to a beam size at the electron beam source of $\sigma_x = 14.9 \pm 0.5\,\mu\text{m}$.

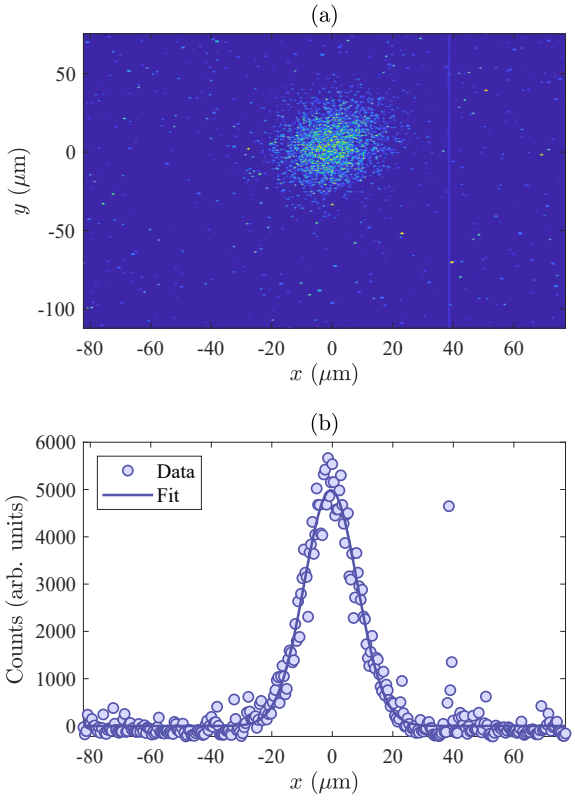


Figure 1: Measured pinhole camera beam profile at 35-BM. This was the smallest beam profile measured using the pinhole camera. (a) Measured pinhole camera image of electron beam. Transverse dimensions $x, y$ are at the optical microscope. (b) Horizontal profile of the image at the scintillator in (a). The fitted width is $\Sigma_x = 12.4 \pm 0.4\,\mu\text{m}$.

Given this beam size, we can determine the electron beam emittance. We substitute the measured value of beam size $\sigma_x = 14.9 \pm 0.5\,\mu\text{m}$, theoretical values of $\beta_\text{x} = 0.84\,\text{m}$, $\eta_\text{x} = 3.67\,\text{mm}$, and $\frac{\Delta E}{E} = 0.156\%$ into Eq. 1. Solving for the horizontal emittance yields $\varepsilon_x = 225 \pm 20\,\text{pm rad}$.

### *Hard X-ray Coherence Measurements*

The transverse coherence and electron beam emittance of the APS-U source were quantitatively characterized at the 3-ID-B beamline using hard X-ray grating interferometry. This technique provides a direct measurement of the source size by analyzing the fringe visibility of interferograms produced by a transmission grating placed in the beam. A detailed description of the method and results for two different machine coupling settings is given in Ref. [7].

The method is based on the van Cittert–Zernike theorem, which relates the spatial coherence of the beam at a measurement plane to the Fourier transform of the source intensity distribution. For a quasi-monochromatic, spatially incoherent source with a Gaussian intensity profile, the transverse coherence function is also Gaussian, and the root-mean-square (RMS) source size $\Sigma$ is related to the transverse coherence length $\xi$ through $\Sigma = (\lambda D)/(2\pi\xi)$, where $\lambda$ is the X-ray wavelength and $D$ is the source-to-measurement-plane distance.

The experimental setup employed a two-dimensional $\pi$-phase checkerboard grating with a 3 µm period, positioned $D = 36.5\,\text{m}$ downstream from the electron waist. Interferograms were recorded at multiple grating-to-detector distances $z$ using a scintillator-coupled sCMOS imaging system with an effective pixel size of 0.65 µm. For each detector position, the fringe visibility was extracted from the amplitude of the first harmonic in the interferogram's Fourier spectrum. The decay of visibility with $z$ was then fitted using:

$$V(z) = V_0 \left| \sin\left[ \frac{\pi \lambda z D}{p_0^2 (z + D)} \right] \right| \exp\left[ -\frac{2\pi^2 z^2 \Sigma^2}{p_0^2 (z + D)^2} \right], \quad (2)$$

where $V_0$ is the baseline visibility factor, $p_0$ is the fringe period at $z = 0$ ($p_0 = 1.5\,\mu\text{m}$ in this setup), and $\Sigma$ is the total RMS source size. This form accounts for both the Talbot self-imaging oscillations and the Gaussian coherence envelope, enabling direct extraction of $\Sigma$ from the measured visibility data, as illustrated in Fig. 2.

Fitting Eq. (2) to the horizontal and vertical visibility curves yielded total source sizes of 13.0 µm and 9.8 µm, respectively. Simulations of single-electron undulator radiation using SRW [8] estimated the intrinsic photon source size to be 4.0 µm in both directions. Removing this contribution in quadrature gave electron source sizes of 12.4 µm (horizontal) and 8.9 µm (vertical).

Beam divergence was measured independently by recording the beam profile at several downstream positions with the grating removed. Linear fits to the beam width versus propagation distance yielded total divergences of 4.9 µrad (horizontal) and 5.6 µrad (vertical). Subtracting the simulated photon divergence of 4.4 µrad gave electron beam divergences of 2.2 µrad and 3.5 µrad, respectively.

Combining the measured electron source sizes and divergences gave electron emittances of $28 \pm 3\,\text{pm rad}$ (horizontal) and $31 \pm 2\,\text{pm rad}$ (vertical). All measurements were performed at a 50 mA beam current under full coupling mode on August 4, 2025. These results are consistent with the storage ring model and confirm a world-record horizontal emittance of $\leq 30\,\text{pm rad}$. Notably, the measurements reported here were conducted on a different day from those presented in [7], demonstrating the repeatability of the technique.

### *Soft X-ray Measurements*

We might intuitively consider the angular distribution of radiation from an electron passing a linear polarisation undulator as a narrow cone, however this is most valid for low undulator harmonics (especially the first harmonic). At high undulator harmonics (e.g. 8-14) this approximation

ISBN: 978-3-95450-261-5 ISSN: 2673-7000 doi: 10.18429/JACoW-NAPAC2025-WEYN03



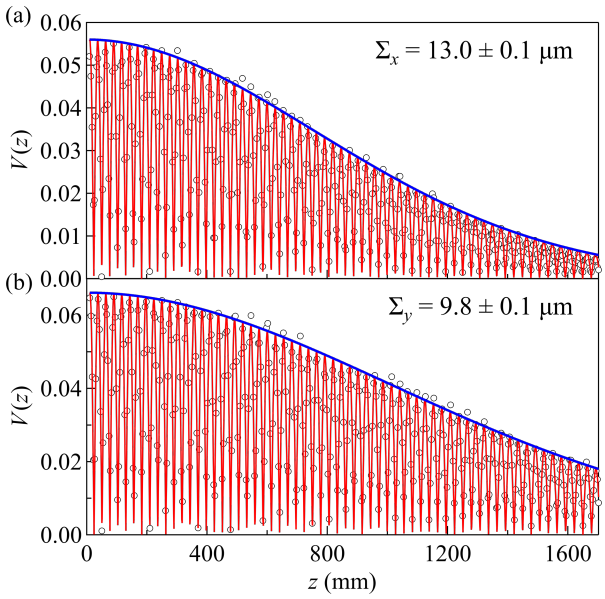


Figure 2: Measured interferogram visibility $V(z)$ (circles) as a function of grating-to-detector distance $z$ for (a) horizontal and (b) vertical directions. Red curves are full fits to Eq. 2, and blue curves show the coherence decay envelope from its exponential term.

breaks down, and a wavefront with narrow angular features is observed [9, 10]. We can use this to measure electron beams passing through the undulator with small emittance in the polarisation plane of the insertion device.

The present measurement employs the Intermediate Energy X-ray beamline at the APS [11]. The photon source of the beamline is an electromagnetic undulator capable of operating in horizontal, vertical or helical polarisation modes [12].

Design values of the parameters of the electron beam at 29-ID in the horizontal plane are summarised in Table 2 [13].

Table 2: Design Electron Beam Parameters at 29-ID [13]

| Parameter | Symbol | Value |
|---|---|---|
| Beam energy | $E$ | 6 GeV |
| Beta function | $\beta_x$ | 5.19 m |
| Emittance | $\varepsilon_x$ | 41.7 pm rad |
| Energy spread | $\frac{\Delta E}{E}$ | 0.135% |
| Dispersion | $\eta_x$ | 0.39 mm |
| Beam size | $\sigma_x$ | 14.7 µm |

The principal diagnostic device in the present study is a pair of DiagOn detectors (for horizontal and vertical polarisation) in the 29-ID beamline, 34.5 m from the insertion device source point [14]. The DiagOn device was operated with a Silicon(111) crystal diffracting at 45°, passing a photon energy of 2796 eV. Hence in order to observe the 8$^{\text{th}}$ harmonic, we configure dthe insertion device to operate with a fundamental photon energy of 349.6 eV (deflection parameter $K = 3.694$). We utilised the DiagOn device to image the profile of undulator radiation at the 8$^{\text{th}}$ harmonic. After measuring and subtracting the imaged bending magnet radiation profile, the measured profile of undulator radiation is plotted in Fig. 3.

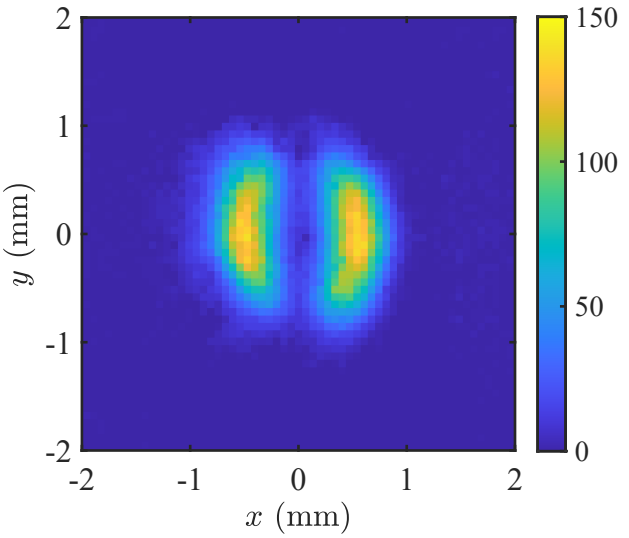


Figure 3: Measured profile of undulator radiation at the 8$^{\text{th}}$ harmonic 2796 eV. The spatial profile was measured using a DiagOn device at 34.5 m distance from the centre of the insertion device. Reproduced under CC-BY 4.0 license from Ref. [15].

The measurement in Fig. 3 was analysed by projecting the measured intensity distribution onto the horizontal axis. This is plotted in Fig. 4 below. Using the parameters in Table 2 corresponding to the experiment, simulate the radiation distribution using SPECTRA [16] and fit to determine the corresponding horizontal emittance. We fit a horizontal emittance of $\varepsilon_x = 47 \pm 8$ pm rad. For comparison, we plot the simulated intensity distribution for $\varepsilon_x = 130$ pm rad corresponding to the emittance for the Key Performance Parameter of the APS-U project.

A particular experimental challenge was encountered during commissioning studies. The measured distribution of radiation exhibited what might be characterised as 'double-peaks', with a small horizontal angular offset between two similar radiation distributions. This was found to correspond to a polarity error in the 'earth field' corrector coil – doubling the magnetic field error corresponding to the earth's magnetic field. Once this polarity error was corrected, the undulator radiation distribution was corrected.

We observe that the measured distribution in Fig. 3 compares favourably with the spatial distribution simulated in 2019 [13]. We have subsequently performed additional measurements to characterise the electron beam in the storage ring using this technique [17].

The beamline front end components were installed during the APS-U installation period. This is illustrated in Fig. 5. The 38-AM enclosure [18] is presently being installed. The enclosure is illustrated in Fig. 6 below.

ISBN: 978-3-95450-261-5 ISSN: 2673-7000 doi: 10.18429/JACoW-NAPAC2025-WEYN03

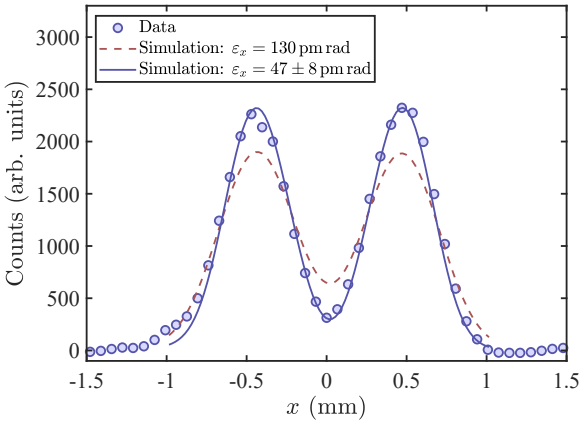


Figure 4: Horizontal projection of measured profile of undulator radiation in Fig. 3. Data shows the horizontal projection of the measured data from Fig. 3. SPECTRA simulations [16] of the expected distribution corresponding to horizontal emittances of $\varepsilon_x = 130$ pm rad, and $\varepsilon_x = 47 \pm 8$ pm rad are fitted. Reproduced under CC-BY 4.0 license from Ref. [15].

Figure 5: 38-AM beamline front end components installed within the storage ring enclosure.

Figure 6: 38-AM beamline enclosure installed to house the endstation instruments.

## FUTURE PINHOLE CAMERA DIAGNOSTIC

The principal diagnostic beamline for measurement of transverse emittance of APS-U will be the 38-AM beam size monitor beamline [19,20]. Construction of the beamline was deferred from the scope of the APS-U project, and so we are continuing to develop that capability for online beam size measurements during accelerator operations. During the APS-U installation period, the core drilling for the beamline penetration was completed. This is illustrated in Figs. 7-8.

Figure 7: 38-AM beamline penetration prior to component installation, viewed from upstream end (inside storage ring tunnel).

Figure 8: 38-AM beamline penetration viewed from outside the storage ring tunnel (prior to enclosure construction).

## EMITTANCE MEASUREMENT AT OTHER LABORATORIES

Emittance measurement and beam size monitoring is performed differently at different laboratories. At MAX-IV,

ISBN: 978-3-95450-261-5 ISSN: 2673-7000 doi: 10.18429/JACoW-NAPAC2025-WEYN03



$\pi$-mode imaging is employed to determine the measured electron beam size [21, 22].

At SIRIUS, pinhole cameras with bending magnet radiation sources are employed to monitor the electron beam size [23, 24].

We see particular similarities between the 38-AM beam size monitor of APS-U with two other similar facilities, notably European Synchrotron Radiation Facility - Extremely Brilliant Source (ESRF-EBS) [25–27] and High Energy Photon Source (HEPS) [28–30]. Both employ hard X-ray pinhole cameras observing a bending magnet as a source point.

## CONCLUSION

Installation of the new low-emittance APS-U electron storage ring was completed. In the present work, photon diagnostic experiments have been used to confirm electron beam size. We have summarised the results of three experiments. During early commissioning, a white beam pinhole camera was implemented at 35-BM, yielding an emittance measurement of $\varepsilon_x = 225 \pm 20$ pm rad before lattice correction was completed. Hard X-ray Talbot interferometry was performed at 3-ID yielding a smallest observed horizontal emittance of $\varepsilon_x = 28 \pm 3$ pm rad [7]. Using undulator radiation characterisation of the Intermediate Energy X-ray beamline, a horizontal emittance of $\varepsilon_x = 47 \pm 8$ pm rad was observed.

The 38-AM beam size monitor beamline is presently under construction, and will be used for routine observation of the electron beam size during storage ring operations. This diagnostic is very similar to that of other similar laboratories also employing pinhole camera beam size monitors.

## ACKNOWLEDGEMENTS

The submitted manuscript has been created by UChicago Argonne, LLC, Operator of Argonne National Laboratory ("Argonne"). Argonne, a U.S. Department of Energy Office of Science Laboratory, is operated under Contract No. DE-AC02-06CH11357. The U.S. Government retains for itself, and others acting on its behalf, a paid-up nonexclusive, irrevocable worldwide license in said article to reproduce, prepare derivative works, distribute copies to the public, and perform publicly and display publicly, by or on behalf of the Government. The Department of Energy will provide public access to these results of federally sponsored research in accordance with the DOE Public Access Plan. http://energy.gov/downloads/doe-public-access-plan

## REFERENCES

[1] J. Kerby, "The Advanced Photon Source Upgrade: A brighter future for X-Ray science", *Synchrotron Radiat. News*, vol. 36, no. 4, pp. 26–27, Jul. 2023. doi:10.1080/08940886.2023.2246816

[2] V. Sajaev *et al.*, "APS Upgrade: Commissioning the world's first light source based on swap-out injection", presented at NAPAC'25, Sacramento, CA, USA, Aug. 2025, paper MOXP02, this conference.

[3] W. E. Norum and B. X. Yang, "A novel FPGA-based bunch purity monitor system at the APS storage ring", in *Proc. PAC'07*, Albuquerque, NM, USA, Jun. 2007, paper FRPMN115, pp. 4384–4386. doi:10.1109/pac.2007.4440014

[4] B. X. Yang, W. E. Norum, S. E. Shoaf, and J. B. Stevens, "Bunch-by-bunch diagnostics at the APS using time-correlated single-photon counting techniques", in *Proc. BIW'10*, Santa Fe, NM, USA, May 2010, paper TUPSM044, pp. 238–242.

[5] K. P. Wootton, W. X. Cheng, G. Decker, N. Sereno, F. Westferro, "Beamline for time domain photon diagnostics at the Advanced Photon Source Upgrade", in *Proc. IBIC'23*, Saskatoon, Canada, Sep. 2023, paper WEP016, pp. 367–371. doi:10.18429/JACoW-IBIC2023-WEP016

[6] K. P. Wootton, E. Aneke, S. Clark, and A. Kastengren, private communication, Jul. 2024.

[7] X. Shi *et al.*, "Measurements of source emittance and beam coherence properties of the upgraded Advanced Photon Source", *J. Synchrotron Radiat.*, vol. 32, no. 5, Sep. 2025, in press.

[8] O. Chubar and P. Elleaume, "Accurate and efficient computation of synchrotron radiation in the near field region", in *Proc. EPAC'98*, Stockholm, Sweden, Jun. 1998, paper THP01G, pp. 1177–1179.

[9] K. P. Wootton *et al.*, "Observation of picometer vertical emittance with a vertical undulator", *Phys. Rev. Lett.*, vol. 109, no. 19, Nov. 2012. doi:10.1103/physrevlett.109.194801

[10] K. P. Wootton, M. J. Boland, and R. P. Rassool, "Measurement of ultralow vertical emittance using a calibrated vertical undulator", *Phys. Rev. Spec. Top. Accel Beams*, vol. 17, no. 11, p. 112802, Nov. 2014. doi:10.1103/physrevstab.17.112802

[11] J. L. McChesney *et al.*, "The intermediate energy X-ray beamline at the APS", *Nucl. Instrum. Methods Phys. Res., Sect. A*, vol. 746, pp. 98–105, May 2014. doi:10.1016/j.nima.2014.01.068

[12] M. S. Jaski *et al.*, "An electromagnetic variably polarizing quasi-periodic undulator", in *Proc. NAPAC'13*, Pasadena, CA, USA, Sep.-Oct. 2013, paper WEPSM09, pp. 1064–1066.

[13] K. P. Wootton, J. L. McChesney, F. M. Rodolakis, N. Sereno, and B. X. Yang, "Transverse emittance measurement using undulator high harmonics for diffraction limited storage rings", in *Proc. IBIC'19*, Malmö, Sweden, Sep. 2019, pp. 674–678. doi:10.18429/JACoW-IBIC2019-THAO04

[14] K. Desjardins *et al.*, "The DiagOn: an undulator diagnostic for SOLEIL low energy beamlines", in *AIP Conf. Proc.*, vol. 879, pp. 1101–1104, Jan. 2007. doi:10.1063/1.2436255

[15] E. Aneke, K. P. Wootton, J. McChesney, H. Zheng, F. Rodolakis, and J. Freeland, "Simulation and measurement of horizontal emittance via undulator high harmonics at the APS-U", *J. Phys. Conf. Ser.*, vol. 3010, no. 1, p. 012032, May 2025. doi:10.1088/1742-6596/3010/1/012032

[16] T. Tanaka and H. Kitamura, "SPECTRA: a synchrotron radiation calculation code", *J. Synchrotron Radiat.*, vol. 8, no. 6, pp. 1221–1228, Oct. 2001. doi:10.1107/s090904950101425x

ISBN: 978-3-95450-261-5 ISSN: 2673-7000 doi: 10.18429/JACoW-NAPAC2025-WEYN03

[17] E. Aneke *et al.*, "Measurement of vertical and horizontal emittance via undulator high harmonics at the APS-U", in *Proc. IPAC'25*, Taipei, Taiwan, Jun. 2025, paper THPM077, to be published.

[18] K. P. Wootton, W. X. Cheng, G. Decker, S. H. Lee, and B. X. Yang, "X-Ray beam size monitor enclosure for the Advanced Photon Source Upgrade", in *Proc. IBIC'20*, Santos, Brazil, Sep. 2020, pp. 34–36. doi:10.18429/JACoW-IBIC2020-TUPP05

[19] B. X. Yang, S. H. Lee, J. W. Morgan, and H. Shang, "High-energy X-Ray pinhole camera for high-resolution electron beam size measurements", in *Proc. IBIC'16*, Barcelona, Spain, Sep. 2016, pp. 504–507. doi:10.18429/JACoW-IBIC2016-TUPG66

[20] K. P. Wootton *et al.*, "Design of the X-Ray beam size monitor for the Advanced Photon Source Upgrade", in *Proc. IPAC'21*, Campinas, Brazil, May 2021, pp. 956–959. doi:10.18429/JACoW-IPAC2021-MOPAB303

[21] J. Breunlin and Å. Andersson, "Emittance diagnostics at the MAX IV 3 GeV storage ring", in *Proc. IPAC'16*, Busan, Korea, May 2016, pp. 2908–2910. doi:10.18429/JACoW-IPAC2016-WEPOW034

[22] J. Breunlin *et al.*, "Diagnostics at the MAX IV 3 GeV storage ring during commissioning", in *Proc. IBIC'16*, Barcelona, Spain, Sep. 2016, pp. 1–5. doi:10.18429/JACoW-IBIC2016-MOAL02

[23] N. Milas, L. Liu, and A. R. D. Rodrigues, "SIRIUS diagnostic beamlines", in *Proc. IPAC'14*, Dresden, Germany, Jun. 2014, pp. 3427–3429. doi:10.18429/JACoW-IPAC2014-THPME082

[24] L. Liu, M. B. Alves, F. H. de Sá, A. C. S. Oliveira, and X. R. Resende, "SIRIUS commissioning results and operation status", in *Proc. IPAC'21*, Campinas, Brazil, May 2021, pp. 13–18. doi:10.18429/JACoW-IPAC2021-MOXA03

[25] L. Torino *et al.*, "Overview on the diagnostics for EBS-ESRF", in *Proc. IBIC'19*, Malmö, Sweden, Sep. 2019, pp. 9–13. doi:10.18429/JACoW-IBIC2019-MOAO03

[26] L. Torino *et al.*, "Beam instrumentation performances through the ESRF-EBS commissioning", in *Proc. IBIC'20*, Santos, Brazil, Sep. 2020, pp. 11–16. doi:10.18429/JACoW-IBIC2020-MOAO04

[27] P. Raimondi *et al.*, "The Extremely Brilliant Source storage ring of the European Synchrotron Radiation Facility", *Commun. Phys.*, vol. 6, p. 82, Apr. 2023. doi:10.1038/s42005-023-01195-z

[28] Y. Sui *et al.*, "Design of HEPS beam diagnostics", in *Proc. IBIC2024*, Beijing, China, Sep. 2024, pp. 11–14. doi:10.18429/JACoW-IBIC2024-TUBI2

[29] D. Zhu *et al.*, "Beam diagnostic beamlines at HEPS storage ring", in *Proc. IBIC2024*, Beijing, China, Sep. 2024, pp. 336–338. doi:10.18429/JACoW-IBIC2024-WEP31

[30] Z. Zhang, "China's "super microscope": High Energy Photon Source enters joint commissioning phase", *Innovation*, vol. 6, no. 9, p. 100946, May 2025. doi:10.1016/j.xinn.2025.100946